Matrix Metalloprotease 2-Responsive Multifunctional Liposomal Nanocarrier for Enhanced Tumor Targeting

Lin Zhu, Pooja Kate, and Vladimir P. Torchilin*

Center for Pharmaceutical Biotechnology and Nanomedicine, Northeastern University, Boston, Massachusetts 02115, United States

ABSTRACT

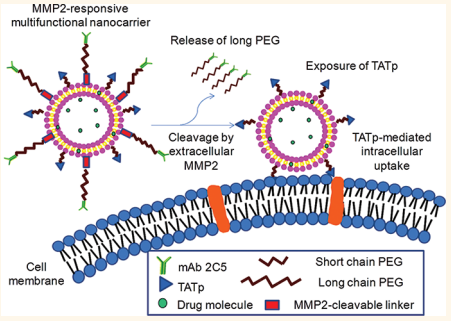

A novel "smart" multifunctional drug delivery system was successfully developed to respond to the up-regulated matrix metalloprotease 2 (MMP2) in the tumor microenvironment and improve cancer cell-specific delivery of loaded drugs. The system represents a surface-functionalized liposomal nanocarrier, for which two functional polyethylene glycol (PEG)—lipid conjugates were synthesized and characterized. The functionalized liposome was further modified with the tumor cell-specific antinucleosome monoclonal antibody (mAb 2C5). In the resulting system, several drug delivery strategies were combined in the same nanocarrier in a simple way and coordinated in an optimal fashion. The functions of the nanocarrier include (i) the hydrophilic and flexible long PEG chains to prevent nanocarrier nonspecific interactions and prolong its circulation time; (ii) a nanoscale size of the system that allows for its passive tumor targeting *via* the enhanced permeability and retention (EPR) effect; (iii) a mAb 2C5 to allow for the specific targeting of tumor cells; (iv) a matrix metalloprotease 2-sensitive bond between PEG and lipid that undergoes cleavage in the tumor by the highly expressed extracellular MMP2 for the removal of PEG chains; (v) cell-penetrating peptide (TATp) triggering of the enhanced intracellular delivery of the system after long-chain PEG removal and exposure of the previously hidden surface-attached TATp. It is shown that such a design can enhance the targetability and internalization of nanocarriers in cancer cells.

KEYWORDS: multifunctional nanocarrier · tumor targeting · stimulus-responsive · matrix metalloprotease 2 · cell-penetrating peptide · monoclonal antibody

The use of pharmaceutical nanocarriers to enhance the *in vivo* efficacy of many drugs has become well-established itself over the past decades.[1] For cancer chemotherapy, site-specific delivery of chemotherapeutic agents to tumor cells is required to prevent undesirable side effects on normal cells, organs, and tissues by toxic drugs and to increase drug bioavailability and the fraction of the drug accumulated in the tumor.[2]

In most cases, the passive targeting strategies that benefit from the longevity of nanocarriers of medicines and the enhanced permeability and retention (EPR) effect at tumors were often not sufficient to accumulate an optimal dose of a drug in the tumor.[2] To enhance targeted delivery of nanopreparations into tumors, the most commonly used strategy has been surface modification of the nanocarriers with targeting moieties including monoclonal antibodies (*e.g.*, anti-transferrin receptor mAb[3] and anti-nucleosome mAb[4,5]), peptides (*e.g.*, Arg-Gly-Asp (RGD)[6]), and small molecules (*e.g.*, folate[7] and galactose[8,9]), which were specific for the antigens or up-regulated receptors on the surface of tumor cells.

The significant internal physiological changes (stimuli) during or after tumor formation including lowered extracellular pH[10] and an altered pattern of the extracellular proteins,[11,12] or the use of external stimuli including magnetic field,[13,14] temperature,[14,15] ultrasound,[16] and light,[17] have been used to design stimulus-responsive pro-drugs or nanocarriers to improve the efficacy of anticancer therapy.

Although the longevity, targeting ligands, and stimuli-responsive moieties of nanomedicines significantly increased the drug disposition in the tumor area, insufficient cellular internalization of nanomedicines can be another significant barrier, especially for macromolecular drugs such as proteins or nucleic acids. To enhance the intracellular uptake, other delivery moieties (cell-penetrating proteins/peptides (CPPs), such as TATp) were used to modify the nanomedicines since they were shown to be efficient in aiding translocation across the plasma membrane.[18]

To date, several of the above strategies had been extensively investigated. However, on

* Address correspondence to v.torchilin@neu.edu.

Received for review February 5, 2012 and accepted March 12, 2012.

Published online March 12, 2012
10.1021/nn300524f

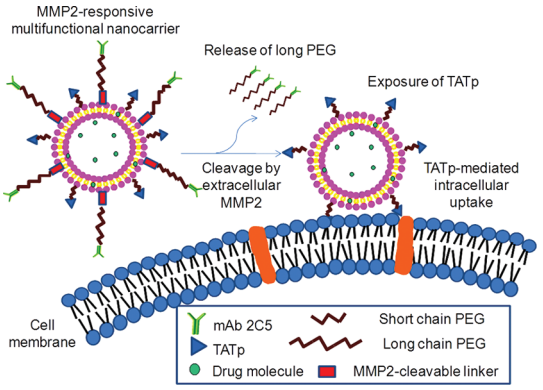

Figure 1. MMP2-responsive multifunctional liposomal nanocarrier and its drug delivery strategy. The multifunctional liposomal nanocarriers are retained in the tumor site due to the EPR effect and the active targeting effect by the anticancer mAb 2C5. The up-regulated MMP2 in the tumor microenvironment cleaves the MMP2-sensitive linker and removes the protective long-chain PEG, resulting in the exposure of TATp for the enhanced cellular internalization.

the basis of the reported data, there is still room for further improvement in terms of drug targetability. Most recently, "dual-"[8−10,14] or even "multi-"[19] functional drug carriers have been proposed and developed, which function together to maximize the efficacy and minimize the drug side effects.[19]

In the current study, we report on the design of a novel multifunctional nanocarrier, which responds to the overexpressed extracellular matrix metalloprotease 2 (MMP2),[11] resulting in the enhanced tumor targetability and internalization. In previous studies, the MMP2 substrates including cleavable peptides had been designed and demonstrated to be degradable in the presence of MMP2.[11,20,21] In our design, the MMP2-cleavable octapeptide (Gly-Pro-Leu-Gly-Ile-Ala-Gly-Gln) was used as a sensitive linker between a liposomal lipid and its long-chain PEG block to serve as a steric shield for the nanoparticle and surface-attached cell-penetrating function (TATp) in the blood. When in the tumor microenvironment, the peptide is expected to be cleaved by the highly expressed extracellular MMP2, leading to the exposure of TATp and enhanced intracellular penetration.

The structure and delivery strategy of the novel multifunctional liposomal nanocarrier are illustrated in Figure 1. Several functions were built into this nanocarrier that were expected to be coordinated in an optimal fashion. The functions of the nanocarrier included (i) the passive tumor targeting by the EPR effect due to longevity imparted by its long PEG chains; (ii) the prevention of the nonspecific intracellular uptake on the way to the tumor by steric shielding of TATp moieties with the long-chain PEG; (iii) the active tumor targeting by a surface-attached cancer-specific monoclonal antibody (mAb 2C5); (iv) the detachment of the long-chain PEG in the tumor due to the cleavage of the MMP2-cleavable linker between the long-chain PEG and the nanocarrier, resulting in the exposure of the cell-penetrating TATp; and (v) the enhanced cellular internalization by TATp-mediated endocytosis.

Here, we described the synthesis of the key functional conjugates, TATp-polyethylene glycol (2000)-1,2-dioctadecanoyl-*sn*-glycero-3-phosphoethanolamine [TATp-PEG(2000)-DSPE] and maleimide-polyethylene glycol (3400)-MMP2 cleavable peptide-1,2-dioleoyl-*sn*-glycero-3-phosphoethanolamine [MAL-PEG(3400)-peptide-DOPE], the preparation and surface modification of the nanocarrier, and the functionality study of MAL-PEG(3400)-peptide-DOPE before and after incorporation into the nanocarrier. We also demonstrate the enhanced *in vitro* cellular uptake of the MMP2-responsive multifunctional nanocarrier by normal and cancer cells as measured with fluorescence-activated cell sorting (FACS).

RESULTS AND DISCUSSION

The incorporation of stimulus-responsive moieties into the targeted delivery systems may achieve precise targetability and controlled release of drug molecules, resulting in the improvement of their therapeutic profiles.[8,10,14] Previously, we described a double-targeted pH-responsive drug delivery system utilizing a lowered pH-cleavable polymer (PEG-Hz-PE) that provided the enhanced cellular internalization of the nanocarriers in the tumor microenvironment.[10]

The altered production of certain extracellular protein in the tumor microenvironment can be significant. MMPs, especially MMP2 and MMP9, are known to be involved in the invasion, progression, and metastasis of most human tumors due to the degradation of the surrounding connective extracellular matrix (ECM).[11] MMP2 is overexpressed in breast cancer, colorectal cancer, lung cancer, liver cancer, prostate cancer, pancreatic cancer, and ovarian cancer.[11] Here, the extracellular MMP2 was used as a stimulus to trigger the enhanced tumor targeting in our newly designed nanocarrier.

Synthesis of the Functional Polymers. The key elements of the suggested nanocarrier were the two functional polymers, TATp-PEG(2000)-DSPE and MAL-PEG(3400)-peptide-DOPE. TATp-PEG(2000)-DSPE was responsible for the enhanced intracellular uptake, while MAL-PEG-(3400)-peptide-DOPE was responsible for the stimulus (up-regulated MMP2 in tumor's ECM) response as well as for the conjugation of the targeting mAb 2C5 with the liposome surface. Both, TATp and MMP2-cleavable peptide have demonstrated the effectiveness in the drug delivery studies.[11,20,22]

Scheme 1A is the synthesis scheme for TATp-PEG-(2000)-DSPE. At pH 6−8, the maleimide group of maleimide-PEG(2000)-DSPE efficiently reacted with the sulfhydryl group of cysteine-modified TAT peptide. After the conjugation and purification, because of the increased hydrophilicity, TATp-PEG(2000)-DSPE remained near the starting point on the thin layer

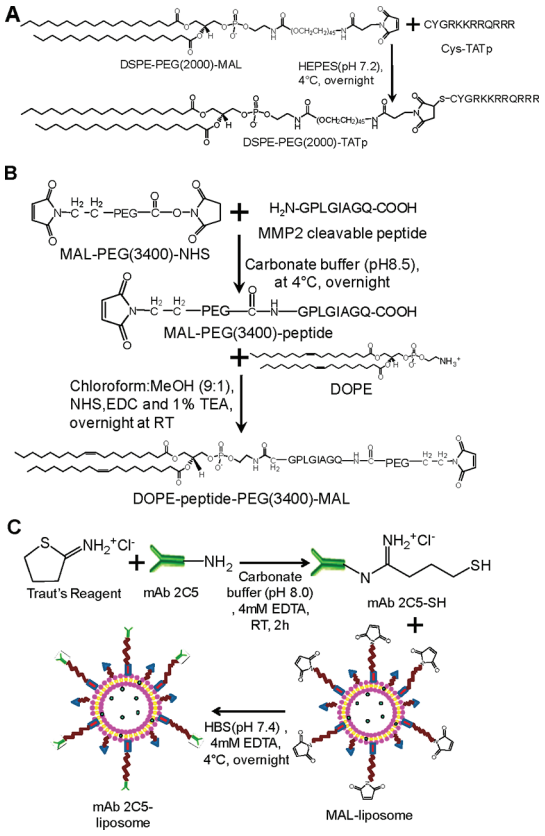

Scheme 1. Synthesis of TATp-PEG(2000)-DSPE (A), MAL-PEG(3400)-peptide-DOPE (B), and surface modification of liposomes with mAb 2C5 (C).

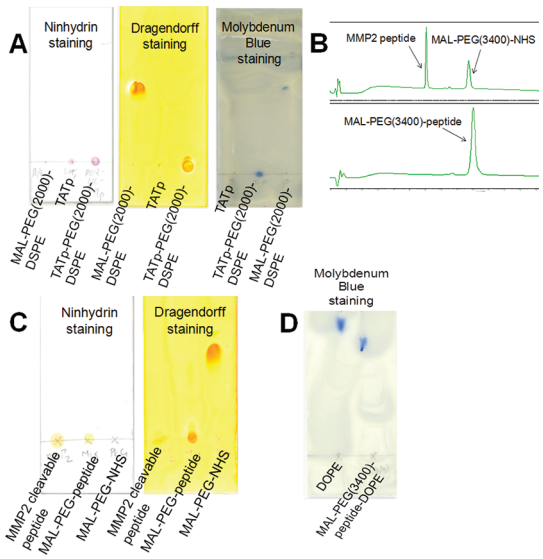

Figure 2. Characterization of TATp-PEG(2000)-DSPE, MAL-PEG(3400)-peptide, and MAL-PEG(3400)-peptide-DOPE. (A) TLC chromatograms of TATp-PEG(2000)-DSPE. (B,C) RP-HPLC and TLC chromatograms of MAL-PEG(3400)-peptide, respectively. (D) TLC chromatogram of MAL-PEG(3400)-peptide-DOPE. The developing solvent for TLC was chloroform/methanol (4/1,v/v). The PEG chains were visualized by Dragendorff's reagent. The peptides were visualized by the ninhydrin spray reagent. The phospholipids were visualized by the molybdenum blue spray reagent. The HPLC chromatograms were collected at 214 nm using gradient solvent conditions: 0−15 min, 5−75% ACN; 15−15.1 min, 75−100% ACN; 15.1−20 min, 100% ACN; 20−20.1 min, 100−5% ACN; 20.1−25 min, 5% ACN, with a flow rate of 1.0 mL/min at room temperature.

chromatography (TLC) plates as visualized by three staining methods (Figure 2A).

Scheme 1B shows the synthesis scheme for MAL-PEG(3400)-peptide-DOPE. To introduce the MMP2-cleavable peptide between the long-chain PEG and the lipid, the primary amine of MMP2-cleavable peptide was first reacted with the *N*-hydroxysuccinimide (NHS) group of the heterobifunctional PEG derivative, MAL-PEG(3400)-NHS, to form an amide bond. After the reaction, the excess of MMP2 peptide and the released NHS were removed by dialysis. The reaction and purification processes were monitored by reverse phase HPLC (RP-HPLC) and TLC. In the HPLC chromatogram (Figure 2B), the peaks of MMP2 peptide (t_R = 9.1 min) and MAL-PEG(3400)-NHS (t_R = 11.8 min) completely disappeared while a new peak of MAL-PEG(3400)-peptide (t_R = 12.1 min) was seen. This change indicated the completion of the product purification. The conjugation reaction and the purification were further confirmed by the TLC (Figure 2C), where the conjugate stayed at the starting point with no migration after staining by either Dragendorff's reagent or ninhydrin spray reagent. The purification procedure precluded a possible reaction between the unreacted peptide and DOPE in the following synthesis. In the second step, the purified MAL-PEG(3400)-peptide was activated by the coupling reagents NHS/EDC and reacted with DOPE *via* the esterification reaction. The product, MAL-PEG(3400)-peptide-DOPE, was separated from the reactants by preparative TLC. The conjugation of MAL-PEG(3400)-peptide with DOPE delayed its migration compared to free DOPE in the TLC plate stained by molybdenum blue spray reagent (Figure 2D). MAL-PEG(3400)-peptide and MAL-PEG(3400)-peptide-DOPE were further confirmed by functionality studies (Figure 3B−F).

Functionality Study of the MMP2-Cleavable Peptide and Its Conjugates. Before liposome preparation, the functionalities of the MMP2-cleavable peptide and its conjugates were evaluated by the enzymatic digestion using active human MMP2. The digest fragments were identified by both RP-HPLC and TLC. The MMP2-cleavable peptide has been reported to be cleaved at the site between glycine and isoleucine and became two small residues (Gly-Pro-Leu-Gly and Ile-Ala-Gly-Gln) in the presence of active MMP2.[11] In the HPLC chromatogram (Figure 3A), two new peaks (t_R = 6 and 8.2 min) were seen, while the peak of the MMP2-cleavable peptide (t_R = 9.2 min) disappeared with the increase of MMP2 concentration. For MAL-PEG(3400)-peptide, only one new peak (Ile-Ala-Gly-Gln) with the retention time of 6 min was shown in the chromatogram after the cleavage because the peak of MAL-PEG(3400)-Gly-Pro-Leu-Gly could not be differentiated from its original form

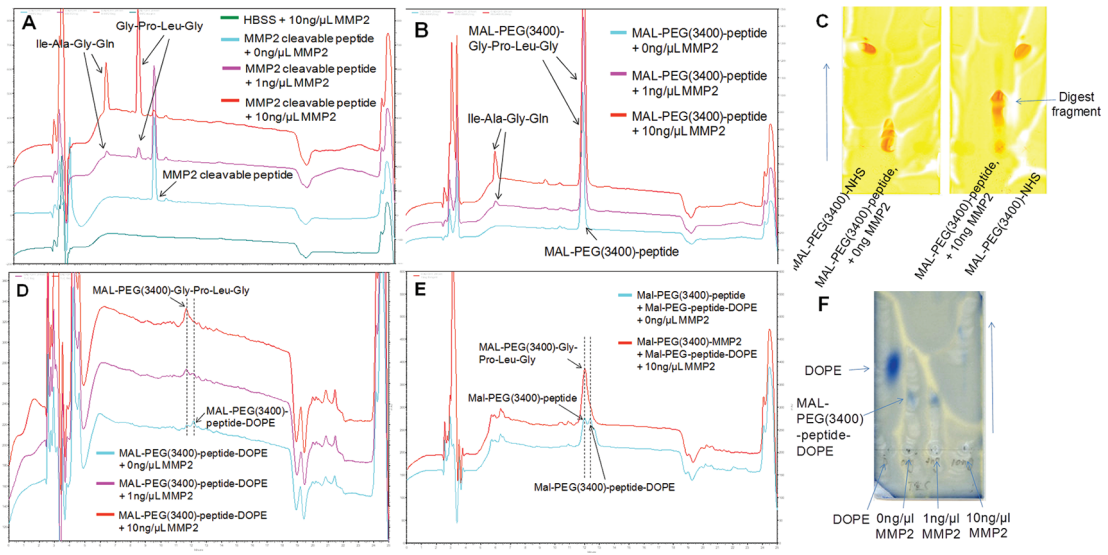

Figure 3. Cleavage assays of the MMP2-cleavable peptide and its conjugates. The peptide and its conjugates were treated with the active human MMP2 at two concentrations, 1 and 10 ng/μL, in HBS at 37 °C for 24 h. The reactions were followed using both RP-HPLC and TLC. Panels A, B, D, and E show the RP-HPLC chromatograms of the MMP2-cleavable peptide (A), MAL-PEG(3400)-peptide (B), MAL-PEG(3400)-peptide-DOPE (D), and the mixture of MAL-PEG(3400)-peptide and MAL-PEG-(3400)-peptide-DOPE (E). Panels C and F show the TLC chromatograms of MAL-PEG(3400)-peptide (C) and MAL-PEG(3400)-peptide-DOPE (F). The conditions for HPLC and TLC were the same as those in the conjugate characterization section.

(MAL-PEG(3400)-peptide) due to their close retention times (around 12 min) (Figure 3B). A similar phenomenon was reported for other PEGylated peptides.[23] The enzymatic cleavage was also supported by the movement of the digest fragments compared to its original form on the TLC plate (Figure 3C). For MAL-PEG(3400)-peptide-DOPE, the peak of the conjugate (t_R = 12.4 min) disappeared, while the peak of PEGylated peptide residue (MAL-PEG-Gly-Pro-Leu-Gly) (t_R = 12 min) was seen after the MMP2 treatment (Figure 3D). To further verify the cleavage, the mixture of MAL-PEG(3400)-peptide-DOPE and MAL-PEG(3400)-peptide was treated with MMP2. After the treatment, the peak of MAL-PEG(3400)-peptide (or MAL-PEG-Gly-Pro-Leu-Gly) was significantly increased, while the peak of MAL-PEG-(3400)-peptide-DOPE disappeared (Figure 3E). On the TLC plate, the spot of MAL-PEG(3400)-peptide-DOPE completely disappeared, while the new spots came out at a location similar to free DOPE when the conjugate was treated with 10 ng/μL of MMP2 (Figure 3F). Figure 3 directly and clearly shows that the MMP2-cleavable peptide did not lose its "cleavability" after the conjugation with both PEG and DOPE at its two ends.

Preparation of the MMP2-Responsive Multifunctional Nanocarrier. The MMP2-responsive liposomes were prepared using the lipid film hydration method followed by extrusion.[10] To incorporate the tumor-targeting moiety, the liposomes were surface-modified with mAb 2C5 *via* a covalent thiol-maleimide linkage (Scheme 1C). The nucleosome-specific mAb 2C5, a subset of natural IgG class antibodies, had been identified as capable of binding a broad spectrum of cancer cells, but not normal cells, *via* their surface-bound nucleosomes originating and released from neighboring apoptotic cancer cells.[4] In tumor inhibition study, the mAb 2C5 induced antibody-dependent cell-mediated cytotoxicity as well as immune responses.[5] The mAb 2C5 has also been successfully used as a tumor cell-targeting ligand for drug delivery with the evidence of the increased cellular uptake and the resulted cytotoxicity of chemotherapeutic drugs in various tumor cells.[5,24] Upon surface modification, the particle size and zeta-potential of the immunoliposomes were determined to be 207.5 $\pm$ 75.5 nm and -10.23 ± 1.21 mV, respectively. It has been suggested that the effective size for the drug delivery systems should be less than 200 nm[25−27] since the threshold vesicle size for the extravasation into a tumor's extracellular space was found to be around 400 nm.[28]

Immunological Activity of the MMP2-Responsive Multifunctional Nanocarrier. The immunological activity of the mAb 2C5 on the multifunctional nanocarrier was determined by ELISA.[10] It was clearly shown that mAb 2C5 and 2C5-modified MMP2-responsive liposomes had similarly high binding affinity with immobilized nucleosomes, while negative controls, IgG and unmodified liposomes, showed no binding (Figure 4A). The high concentration of mAb 2C5 saturated the plate and could not present its real binding affinity (Figure 4A). Therefore, the near linear range (0−1.25 μg/mL of mAb 2C5) was selected to compare the binding affinities of the liposomal formulations (Figure 4B). After the treatment with MMP2, 2C5-PEG(3400)-Gly-Pro-Leu-Gly was liberated from the nanocarrier due to the cleavage of MMP2-cleavable linker between PEG(3400) and DOPE. The liberated 2C5-PEG(3400)-Gly-Pro-Leu-Gly stayed with the nanocarrier, which

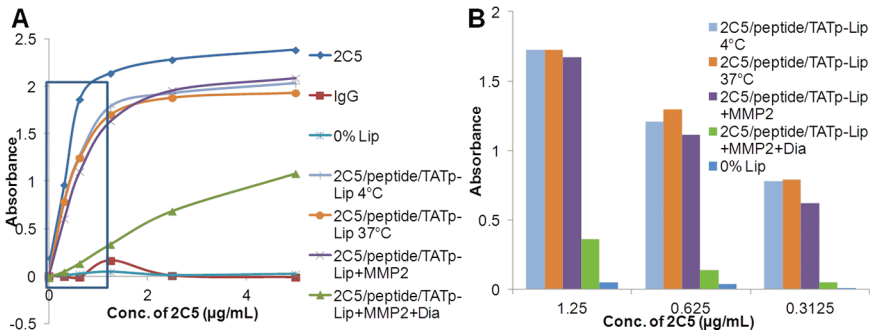

Figure 4. Immunological activity of the MMP2-responsive multifunctional liposomal nanocarrier. To study the binding affinities of the liposomal nanocarriers toward nucleosomes, a series of diluted samples were measured using an ELISA assay. The samples included mAb 2C5, IgG, unmodified liposomes (0% Lip), the MMP2-responsive multifunctional nanocarriers incubated at 4 °C (2C5/peptide/TATp-Lip 4 °C) and at 37 °C (2C5/peptide/TATp-Lip 37 °C), MMP2-treated MMP2-responsive multifunctional nanocarriers (2C5/peptide/TATp-Lip+MMP2), and MMP2-treated MMP2-responsive multifunctional nanocarriers followed by dialysis (2C5/peptide/TATp-Lip+MMP2+Dia). (A) UV absorbances of all samples in the ELISA assay. (B) UV absorbance of the liposomal formulations only in the near linear range from (A). Abbreviation: 2C5, mAb 2C5; peptide, MMP2-cleavable peptide; TATp, TAT peptides; Lip, liposomes; Dia, dialysis.

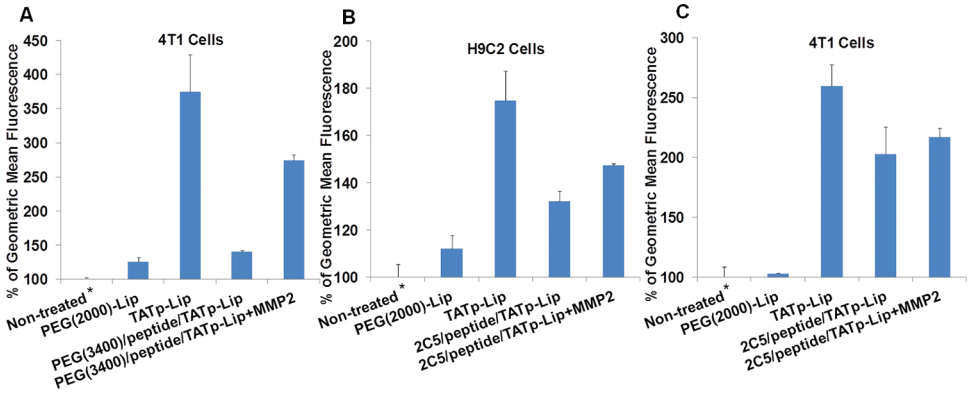

Figure 5. FACS analysis of the interaction of Rh-PE-labeled MMP2-responsive multifunctional liposomal nanocarrier with 4T1 and H9C2 cells. (A) 4T1 cells incubated (for 1 h before FACS analysis) with 1% mPEG(2000)-modified liposomes [PEG(2000)-Lip], 1% TATp-modified liposomes (TATp-Lip), and MMP2-responsive nanocarriers [PEG(3400)/peptide/TATp-Lip] with or without pretreatment with MMP2. (B) H9C2 cells incubated with PEG(2000)-Lip, TATp-Lip, and MMP2-responsive multifunctional nanocarriers (2C5/peptide/TATp-Lip) with or without pretreatment with MMP2. (C) 4T1 cells incubated with the same liposome preparations as in (B). The geometric mean of the fluorescence for nontreated cells was defined as 100% (*). Abbreviation: 2C5, mAb 2C5; peptide, MMP2-cleavable peptide; TATp, TAT peptides; Lip, liposomes; Rh-PE, 1,2-dioleoyl-*sn*-glycero-3-phosphoethanolamine-*N*-(lissamine rhodamine B sulfonyl) (ammonium salt).

showed a binding affinity similar to that of the non-treated nanocarriers. However, the binding affinity of the MMP2-responsive multifunctional nanocarrier was significantly decreased (by 21% at 1.25 μg/mL, 12% at 0.625 μg/mL, and 7.6% at 0.3125 μg/mL) after the liberated 2C5-PEG(3400)-Gly-Pro-Leu-Gly was removed using a floating dialysis device (MWCO 300 000 Da) (Figure 4B). The remaining binding activity of the samples might, most probably, come from the incomplete cleavage of the peptide linker due to the steric hindrance of the protective PEG(3400) moiety.[8,29] Firm adsorption of the cleaved high MW 2C5-PEG-peptide moiety not completely overcome by dialysis is also possible. However, the effect of remaining 2C5-PEG moieties was negligible as follows from the data shown in Figures 4B and 5. The ELISA results suggested that mAb 2C5 was successfully conjugated to MAL-PEG(3400)-peptide-DOPE on the surface of nanocarriers *via* the MMP2-cleavable linker and did not lose its immunological activity. The data also confirmed that the MMP2-cleavable conjugate retained its function after incorporation into the nanocarriers.

Cellular Uptake and FACS. To evaluate this novel delivery system, *in vitro* cellular uptake tests were performed with mouse breast cancer cells (4T1) and normal rat cardiomyocytes (H9C2). The cells treated with various fluorescently labeled systems at different conditions were analyzed by FACS (Figure 5). All cells treated with liposomal formulations containing 1% TATp had significantly higher liposome uptake (geometric mean fluorescence) than untreated control cells, while the fluorescence of the cells treated with liposomes containing only PEG(2000) was equivalent to that of untreated cells for both normal and tumor cells. These data confirmed the previous observations that PEG chains inhibit the interaction between the

PEGylated nanocarriers and cells resulting in the low internalization.[10] At the cellular level, PEGylation had also been found to interfere with intracellular events, such as endosomal escape,[30] which could impair the expected clinical outcomes associated with both the passive and active targeting.

TATp-modified liposomes demonstrated the highest cellular uptake in both cell lines (Figure 5). The TATp is known to enhance the intracellular delivery of various cargoes, including both molecules and particles, *via* either endocytosis or macropinocytosis.[10,22] It was found earlier that the direct electrostatic interaction between positive residues of the TATp and negatively charged cell-surface proteoglycans or glycosaminoglycans was required for the internalization, regardless of the mechanisms involved.[18] Liposomes containing, in addition to TATp, protective long-chain PEG(3400) moieties to shield the TATp groups demonstrated a level of uptake very close to that of the liposomes modified with only PEG(2000). This is quite understandable since the presence of PEG(3400) prevents TATp contact with cells. However, when such preparations containing PEG(3400)-peptide-DOPE were first treated with MMP-2 (which should degrade the peptide sequence between DOPE and PEG residues and eliminate PEG blocks from the surface of liposomes) and then incubated with cells, the uptake level characteristic for TATp-modified liposomes was restored to a significant extent and confirmed the deshielding of TATp and its effective interaction with cells resulting in good liposome uptake (see the data with 4T1 cells in Figure 5A). Thus, both key functions of our system, PEG-mediated TATp shielding and MMP2 sensitivity that deblocks this shielding work and should minimize its nonspecific uptake when en route to a tumor and maximize its penetration of cancer cells when in a tumor microenvironment with locally enhanced MMP2 activity.

An additional interesting observation was made when these systems were additionally modified with cancer-specific mAb 2C5 *via* the same MMP2-sensitive spacer PEG(3400)-peptide-DOPE. In H9C2 cells, the incorporation of 1% 2C5-PEG(3400)-peptide-DOPE into TATp-liposomes (2C5/peptide/TATp-Lip), as expected, significantly decreases the efficiency of the cellular uptake (which still remains higher than that for PEG only modified liposomes probably because of some additional protein-mediated interaction). The pretreatment of such MMP2-responsive multifunctional nanocarriers with MMP2 eliminated the 2C5-PEG-block, exposed TATp, and again increased the cellular uptake (Figure 5B). The specific 2C5-mediated interaction should not play any role with normal cells since normal H9C2 cells do not bear sufficient surface nucleosomes.

In 4T1 cancer cells, however, the specific cellular uptake mediated by mAb 2C5 is high enough on its own[24] and comparable with the uptake provoked by TATp upon its deshielding by the effect of MMP2 (Figure 5C). From a practical point, it could mean that the MMP2-sensitive long-circulating systems may not need an additional modification with cancer-specific antibody, and the EPR effect in combination with TATp plus MMP2 sensitivity could provide sufficient intracellular delivery of anticancer drugs for a strong therapeutic effect. This issue will be additionally investigated in our ongoing *in vivo* experiments.

On the basis of the current data, we can propose that the following chain of events describes the behavior of our system *in vivo*. After the intravenous administration, the PEGylated 200 nm MMP2-responsive multifunctional nanocarriers will demonstrate a prolonged circulation time sufficient for their accumulation in the tumor[2] *via* the EPR effect.[28] A specific ligand (such as mAb 2C5) attached to the surface of the nanocarrier provides an additional recognition and binding within tumors (but not with healthy tissues), resulting in tumor cell-specific targeting. Upon the accumulation at the tumor site, the up-regulated MMP2 in the tumor microenvironment will cleave the MMP2-sensitive peptide linker in surface-attached conjugates and will result in the elimination of the long PEG chains and exposure of TATp moieties on the surface of the nanocarrier to allow enhanced cellular internalization of such a drug-loaded system by tumor cells. Thus, the combination of several such drug delivery strategies within this novel nanocarrier should allow for precise and effective tumor targeting and intracellular delivery.

CONCLUSION

In the current study, we successfully synthesized and characterized two novel functional polymers for surface modification of pharmaceutical nanocarriers. By using these polymers, a novel multifunctional stimulus-sensitive nanocarrier was developed, which accumulates in tumors and specifically targets cancer cells, responds to the up-regulated extracellular MMP2 in tumors, and provides enhanced cellular internalization *via* a cell penetration function (TATp), which becomes exposed and active when the nanocarrier is in a tumor microenvironment.

MATERIALS AND METHODS

Materials. Maleimide-polyethylene glycol (3400)-*N*-hydroxysuccinimide ester (MAL-PEG(3400)-NHS) was purchased from Creative PEGWorks (Winston Salem, NC). L-α-Phosphatidylcholine (egg PC), 1,2-distearoyl-*sn*-glycero-3-phosphoethanolamine-*N*-[methoxy(polyethylene glycol)-2000] (ammonium

salt) (mPEG(2000)-DSPE), 1,2-distearoyl-*sn*-glycero-3-phosphoethanolamine-*N*-[maleimide(polyethylene glycol)-2000] (MAL-PEG(2000)-DSPE), 1,2-dioleoyl-*sn*-glycero-3-phosphoethanolamine (DOPE), and 1,2-dioleoyl-*sn*-glycero-3-phosphoethanolamine-*N*-(lissamine rhodamine B sulfonyl) (ammonium salt) (Rh-PE) were purchased from Avanti Polar Lipids, Inc. (Alabaster, AL). Cysteine-modified TAT (Cys-TATp) and MMP2-cleavable peptides were synthesized by the Tufts University Core Facility (Boston, MA). Traut's reagent, Zeba Desalt spin column (MWCO 7000 Da, 2 mL), *N*-hydroxysuccinimide (NHS), and triethylamine (TEA) were purchased from Thermo Fisher Scientific (Rockford, IL). 1-Ethyl-3-[3-dimethylaminopropyl]carbodiimide hydrochloride (EDC), ninhydrin spray reagent, and molybdenum blue spray reagent were from Sigma-Aldrich Chemicals (St. Louis, MO). Trifluoroacetic acid (TFA), chloroform, and methanol were purchased from Fisher Scientific (Fair Lawn, NJ). Human active MMP2 protein (MW 66 000 Da) and TLC plate (silica gel 60 F_{254}) were from EMD Biosciences (La Jolla, CA). Dialysis tubing (MWCO 2000 Da) and the floating dialysis device (MWCO 300 000 Da) were purchased from Spectrum Laboratories, Inc. (Houston, TX). Dulbecco's modified Eagle's medium (DMEM), penicillin/streptomycin solution (PS) (100×), and trypsin-EDTA were from Invitrogen Corporation (Carlsbad, CA). FBS was purchased from Atlanta Biologicals (Lawrenceville, GA). IgG was obtained from Serologicals Proteins, Inc. (Kankakee, IL). The goat anti-mouse IgG peroxidase conjugate was purchased from ICN Biomedicals, Inc. (Aurora, OH). The enhanced Kblue TMB peroxidase substrate was from Neogen Corporation (Lexington, KY). The mAb 2C5 was produced in ascites *via* the i.p. injection of hybridoma cells into pristine-primed 4 week old BALB/c male mice. The production and purification of the mAb 2C5 were carried out by Harlan Bioproducts (Indianapolis, IN) using the cells from our laboratory.

Synthesis, Purification, and Characterization of TATp-PEG(2000)-DSPE. To synthesize TATp-PEG(2000)-DSPE, 4.2 mg of cysteine-modified TATp (Cys-Tyr-Gly-Arg-Lys-Lys-Arg-Arg-Gln-Arg-Arg-Arg) and 6 mg of MAL-PEG(2000)-DSPE were dissolved in 1.5 mL of pH 7.2 HEPES buffer. The reaction mixture was stirred at 4 °C under nitrogen protection overnight (Scheme 1A). The excess of Cys-TATp was removed by dialysis (MWCO 2000 Da) against distilled water. The reaction and purification processes were monitored by TLC with a developing solvent of chloroform/methanol mixture (4/1,v/v). The TLC plates were then visualized by Dragendorff's reagent (a self-preparation using a U.S. Pharmacopeia protocol) staining for the PEG chains, by ninhydrin spray reagent staining for the peptides, and by molybdenum blue spray reagent staining for the phospholipids.

Two-Step Synthesis, Purification, And Characterization of MAL-PEG-(3400)-Peptide-DOPE. In the first step (Scheme 1B), the MMP2-cleavable peptide (NH_2-Gly-Pro-Leu-Gly-Ile-Ala-Gly-Gln-COOH) and MAL-PEG(3400)-NHS (1.2:1, molar ratio) were mixed and stirred in the carbonate buffer (pH 8.5) at 4 °C overnight. The excess of peptides was removed by dialysis (MWCO 2000 Da) against distilled water. MAL-PEG(3400)-peptide was identified by RP-HPLC on a reverse phase C18 column (250 mm × 4.6 mm, Alltech) by the LaChrom Elite HPLC system (Hitachi). The chromatograms were collected at 214 nm using gradient solvent conditions. The chromatographic conditions used for the analysis were as follows: solvent A, 0.1% TFA in acetonitrile (ACN); solvent B, 0.1% TFA in water; 0−15 min, 5−75% ACN; 15−15.1 min, 75−100% ACN; 15.1−20 min, 100% ACN; 20−20.1 min, 100−5% ACN; 20.1−25 min, 5% ACN, with a flow rate of 1.0 mL/min at room temperature. The product was freeze-dried for the next step.

In the second step (Scheme 1B), MAL-PEG(3400)-peptide was activated with a 20-fold molar excess of NHS/EDC (1:1, molar ratio) in an anhydrous chloroform/methanol mixture (9:1, v/v) for 2 h. The activated MAL-PEG-peptide was then reacted with excess DOPE in the presence of 1% of TEA under nitrogen protection at room temperature overnight. The reaction was monitored using TLC followed by the molybdenum blue spray reagent staining. MAL-PEG(3400)-peptide-DOPE was purified by preparative TLC (same conditions as analytical TLC).

Cleavage of the MMP2-Cleavable Peptide and Its Functional Conjugates. The functions of MMP2-cleavable peptide and its conjugates were evaluated by enzymatic digestion using the active human MMP2. Briefly, 1 mg/mL of the MMP2-cleavable peptide, MAL-PEG(3400)-peptide, and MAL-PEG(3400)-peptide-DOPE was incubated individually with MMP2 in pH 7.4 HEPES-buffered saline (HBS) (50 mM HEPES, 150 mM NaCl) containing 10 mM $CaCl_2$ at 37 °C for 24 h. Two final concentrations (1 and 10 ng/μL) of MMP2 in the digestion reaction were used for each compound. The digestion fragments were identified by RP-HPLC (as above) and confirmed by TLC with Dragendorff's reagent and molybdenum blue spray reagent staining.

Preparation of Liposomes. To prepare the MMP2-responsive liposomes [PEG(3400)/peptide/TATp-Lip], the lipid mixture of egg PC (60 mol %), cholesterol (38 mol %), TATp-PEG(2000)-DSPE (1 mol %), and MAL-PEG(3400)-peptide-DOPE (1 mol %) was dissolved in chloroform. The lipid film was formed by rotary evaporation and overnight freeze-drying. The film was hydrated with HBS at room temperature for 20 min. The lipid dispersion was extruded 40 times through polycarbonate filters (pore size 200 nm) using a microextruder (Avanti). For mPEG(2000)-modified liposomes (PEG(2000)-Lip), egg PC (60 mol %), cholesterol (39 mol %), and mPEG(2000)-DSPE (1 mol %) were used to make the lipid film. For TATp-modified liposomes (TATp-Lip), egg PC (60 mol %), cholesterol (39 mol %), and TATp-PEG(2000)-DSPE (1 mol %) were used to make the lipid film. The unmodified liposomes (0% Lip) contained only egg PC (60 mol %) and cholesterol (40 mol %). To follow liposome-to-cell interactions, Rh-PE (0.5 mol %) was added to the liposomal formulations.

Surface Modification of the MMP2-Responsive Liposomes with mAb 2C5. The mAb 2C5 was first thiolated by Traut's reagent according to the manufacturer's manual. Briefly, mAb 2C5 reacted with Traut's reagent in pH 8.0 carbonate buffer containing 4 mM EDTA at the molar ratio of 1/20 at room temperature for 1 h. The thiolated mAb 2C5 was purified using a Zeba Desalt spin column. To covalently attach mAb 2C5 to the MMP2-responsive liposomes, the liposomes were incubated with thiolated mAb 2C5 at the molar ratio of 20 maleimide groups per antibody. The reaction was carried out in HBS, pH 7.4, containing 4 mM EDTA at 4 °C overnight (Scheme 1C). The free mAb 2C5 was removed by dialysis with a floating dialysis device (MWCO 300 000 Da) against HBS. The particle size and zeta-potential of the nanocarriers were measured using a Coulter N4 Plus submicrometer particle analyzer (Beckman Coulter Inc., Watertown, MA) and a Zeta Plus zeta-potential analyzer (Brookhaven Instruments Corporation, Holtsville, NY), respectively.

ELISA. To evaluate the immunological activity of mAb 2C5 and the cleavable property of the MMP2-sensitive linker on the MMP2-responsive multifunctional nancocarriers, an ELISA was performed. Briefly, a 96-well microplate was precoated with 50 μL/well of 40 μg/mL poly-L-lysine solution in pH TRIS-buffered saline (TBS), pH 7.4, at 4 °C overnight. The plate was washed three times by TBST (TBS containing 0.05% w/v Tween-20) and incubated with 200 μL of TBST-casein solution (containing 2 mg/mL casein) at room temperature for 1 h to block the nonspecific binding. Then the plate was coated with 50 μL of 40 μg/mL mononucleosomes (the water-soluble fraction of calf thymus nucleohistone) in TBST-casein at room temperature for 1 h. After washing the plate with TBST, 50 μL of a series of diluted samples (mAb 2C5, IgG, unmodified liposomes, mAb 2C5-modified liposomes (at 4 and 37 °C) and MMP2-treated mAb 2C5-modified liposomes (with and without dialysis, MWCO 300 000 Da)) was loaded into the plate and incubated at room temperature for 1 h. The samples were removed, and the plate was thoroughly washed before incubation with 50 μL/well of 1:5000 dilution of goat anti-mouse IgG peroxidase conjugate in TBST-casein at room temperature for 1 h. Each well was incubated with 100 μL of the enhanced K-blue TMB peroxidase substrate at room temperature for 15 min. Finally, the microplate was read at 620 nm with the reference filter of 492 nm using a Labsystems Multiscan MCC/340 microplate reader (Thermo Fisher Scientific).

Cellular Uptake and FACS. 4T1 and H9C2 cells were maintained in a complete growth medium containing DMEM supplemented with 10% FBS, 100 IU/mL penicillin, and 100 μg/mL

streptomycin at 37 °C in a 5% CO_2 humidified atmosphere. Before experiments, the cells were seeded in six-well culture plates at the density of 1×10^5 cells/well. After 48 h, the cells were washed twice with pH 7.4 PBS and then treated with various Rh-PE-labeled liposomes [PEG(2000)-Lip, TATp-Lip, and the MMP2-responsive nanocarriers (PEG(3400)/peptide/TATp-Lip) and MMP2-responsive multifunctional nanocarriers (2C5/peptide/TATp-Lip) with/without preincubation with 5 ng/μL of MMP2] in 1 mL/well of the serum-free medium. After 1 h incubation with Rh-PE-labeled liposomes, the medium was removed, and the cells were washed with the serum-free medium three times. Then, the cells were trypsinized and collected by centrifugation at 3000 rpm for 4 min. After washing with ice-cold PBS, the cell pellet was resuspended in 100 μL of PBS and applied immediately on a BD FACS Calibur flow cytometer (BD Biosciences, San Jose, CA). The cells were gated upon acquisition using forward *versus* side scatter to exclude debris and dead cells. The data were collected (10 000 cell counts) and analyzed with BD Cell Quest Pro Software.

Statistical Analysis. Data were presented as the mean ± standard deviation (SD). The difference between any two groups was determined by ANOVA. $P < 0.05$ was considered statistically significant.

Conflict of Interest: The authors declare no competing financial interest.

Acknowledgment. The authors thank Drs. Rupa Sawant, Swati Biswas, and Federico Perche for their advice in the experiments, and Drs. William C. Hartner, Tatyana Levchenko, and Alexander Koshkaryev for their help in manuscript preparation. This work was supported by the NIH Grant 1R01CA121838 to V.P.T.

REFERENCES AND NOTES

1. Torchilin, V. P. Recent Advances with Liposomes as Pharmaceutical Carriers. *Nat. Rev. Drug Discovery* **2005**, *4*, 145–160.
2. Torchilin, V. P. Targeted Pharmaceutical Nanocarriers for Cancer Therapy and Imaging. *AAPS J.* **2007**, *9*, E128–E147.
3. Friden, P. M.; Walus, L. R.; Musso, G. F.; Taylor, M. A.; Malfroy, B.; Starzyk, R. M. Anti-Transferrin Receptor Antibody and Antibody–Drug Conjugates Cross the Blood–Brain Barrier. *Proc. Natl. Acad. Sci. U.S.A.* **1991**, *88*, 4771–4775.
4. Iakoubov, L. Z.; Torchilin, V. P. A Novel Class of Antitumor Antibodies: Nucleosome-Restricted Antinuclear Autoantibodies (ANA) from Healthy Aged Nonautoimmune Mice. *Oncol. Res.* **1997**, *9*, 439–446.
5. Lukyanov, A. N.; Elbayoumi, T. A.; Chakilam, A. R.; Torchilin, V. P. Tumor-Targeted Liposomes: Doxorubicin-Loaded Long-Circulating Liposomes Modified with Anti-Cancer Antibody. *J. Controlled Release* **2004**, *100*, 135–144.
6. Ruoslahti, E. RGD and Other Recognition Sequences for Integrins. *Annu. Rev. Cell. Dev. Biol.* **1996**, *12*, 697–715.
7. Gabizon, A.; Horowitz, A. T.; Goren, D.; Tzemach, D.; Mandelbaum-Shavit, F.; Qazen, M. M.; Zalipsky, S. Targeting Folate Receptor with Folate Linked to Extremities of Poly(ethylene glycol)-Grafted Liposomes: *In Vitro* Studies. *Bioconjugate Chem.* **1999**, *10*, 289–298.
8. Zhu, L.; Ye, Z.; Cheng, K.; Miller, D. D.; Mahato, R. I. Site-Specific Delivery of Oligonucleotides to Hepatocytes after Systemic Administration. *Bioconjugate Chem.* **2008**, *19*, 290–298.
9. Zhu, L.; Mahato, R. I. Targeted Delivery of siRNA to Hepatocytes and Hepatic Stellate Cells by Bioconjugation. *Bioconjugate Chem.* **2010**, *21*, 2119–2127.
10. Sawant, R. M.; Hurley, J. P.; Salmaso, S.; Kale, A.; Tolcheva, E.; Levchenko, T. S.; Torchilin, V. P. "SMART" Drug Delivery Systems: Double-Targeted pH-Responsive Pharmaceutical Nanocarriers. *Bioconjugate Chem.* **2006**, *17*, 943–949.
11. Mansour, A. M.; Drevs, J.; Esser, N.; Hamada, F. M.; Badary, O. A.; Unger, C.; Fichtner, I.; Kratz, F. A New Approach for the Treatment of Malignant Melanoma: Enhanced Antitumor Efficacy of an Albumin-Binding Doxorubicin Prodrug That Is Cleaved by Matrix Metalloproteinase 2. *Cancer Res.* **2003**, *63*, 4062–4066.
12. Basel, M. T.; Shrestha, T. B.; Troyer, D. L.; Bossmann, S. H. Protease-Sensitive, Polymer-caged Liposomes: A Method for Making Highly Targeted Liposomes Using Triggered Release. *ACS Nano* **2011**, *5*, 2162–2175.
13. Alexiou, C.; Arnold, W.; Klein, R. J.; Parak, F. G.; Hulin, P.; Bergemann, C.; Erhardt, W.; Wagenpfeil, S.; Lubbe, A. S. Locoregional Cancer Treatment with Magnetic Drug Targeting. *Cancer Res.* **2000**, *60*, 6641–6648.
14. Zhu, L.; Huo, Z.; Wang, L.; Tong, X.; Xiao, Y.; Ni, K. Targeted Delivery of Methotrexate to Skeletal Muscular Tissue by Thermosensitive Magnetoliposomes. *Int. J. Pharm.* **2009**, *370*, 136–143.
15. Needham, D.; Anyarambhatla, G.; Kong, G.; Dewhirst, M. W. A New Temperature-Sensitive Liposome for Use with Mild Hyperthermia: Characterization and Testing in a Human Tumor Xenograft Model. *Cancer Res.* **2000**, *60*, 1197–1201.
16. Schroeder, A.; Honen, R.; Turjeman, K.; Gabizon, A.; Kost, J.; Barenholz, Y. Ultrasound Triggered Release of Cisplatin from Liposomes in Murine Tumors. *J. Controlled Release* **2009**, *137*, 63–68.
17. Wan, Y.; Angleson, J. K.; Kutateladze, A. G. Liposomes from Novel Photolabile Phospholipids: Light-Induced Unloading of Small Molecules As Monitored by PFG NMR. *J. Am. Chem. Soc.* **2002**, *124*, 5610–5611.
18. Torchilin, V. P.; Rammohan, R.; Weissig, V.; Levchenko, T. S. TAT Peptide on the Surface of Liposomes Affords Their Efficient Intracellular Delivery Even at Low Temperature and in the Presence of Metabolic Inhibitors. *Proc. Natl. Acad. Sci. U.S.A.* **2001**, *98*, 8786–8791.
19. Torchilin, V. P. Multifunctional Nanocarriers. *Adv. Drug Delivery Rev.* **2006**, *58*, 1532–1555.
20. Kratz, F.; Drevs, J.; Bing, G.; Stockmar, C.; Scheuermann, K.; Lazar, P.; Unger, C. Development and *In Vitro* Efficacy of Novel MMP2 and MMP9 Specific Doxorubicin Albumin Conjugates. *Bioorg. Med. Chem. Lett.* **2001**, *11*, 2001–2006.
21. Terada, T.; Iwai, M.; Kawakami, S.; Yamashita, F.; Hashida, M. Novel PEG-Matrix Metalloproteinase-2 Cleavable Peptide-Lipid Containing Galactosylated Liposomes for Hepatocellular Carcinoma-Selective Targeting. *J. Controlled Release* **2006**, *111*, 333–342.
22. Torchilin, V. P.; Levchenko, T. S.; Rammohan, R.; Volodina, N.; Papahadjopoulos-Sternberg, B.; D'Souza, G. G. Cell Transfection *in Vitro* and *in Vivo* with Nontoxic TAT Peptide-Liposome-DNA Complexes. *Proc. Natl. Acad. Sci. U.S.A.* **2003**, *100*, 1972–1977.
23. Hinds, K.; Koh, J. J.; Joss, L.; Liu, F.; Baudys, M.; Kim, S. W. Synthesis and Characterization of Poly(ethylene glycol)–Insulin Conjugates. *Bioconjugate Chem.* **2000**, *11*, 195–201.
24. Elbayoumi, T. A.; Torchilin, V. P. Enhanced Cytotoxicity of Monoclonal Anticancer Antibody 2C5-Modified Doxorubicin-Loaded PEGylated Liposomes against Various Tumor Cell Lines. *Eur. J. Pharm. Sci.* **2007**, *32*, 159–168.
25. Klibanov, A. L.; Maruyama, K.; Beckerleg, A. M.; Torchilin, V. P.; Huang, L. Activity of Amphipathic Poly(ethylene glycol) 5000 To Prolong the Circulation Time of Liposomes Depends on the Liposome Size and Is Unfavorable for Immunoliposome Binding to Target. *Biochim. Biophys. Acta* **1991**, *1062*, 142–148.
26. Awasthi, V. D.; Garcia, D.; Goins, B. A.; Phillips, W. T. Circulation and Biodistribution Profiles of Long-Circulating PEG-Liposomes of Various Sizes in Rabbits. *Int. J. Pharm.* **2003**, *253*, 121–132.
27. Peer, D.; Karp, J. M.; Hong, S.; Farokhzad, O. C.; Margalit, R.; Langer, R. Nanocarriers as an Emerging Platform for Cancer Therapy. *Nat. Nanotechnol.* **2007**, *2*, 751–760.
28. Yuan, F.; Dellian, M.; Fukumura, D.; Leunig, M.; Berk, D. A.; Torchilin, V. P.; Jain, R. K. Vascular Permeability in a Human Tumor Xenograft: Molecular Size Dependence and Cutoff Size. *Cancer Res.* **1995**, *55*, 3752–2756.
29. Klibanov, A. L.; Maruyama, K.; Torchilin, V. P.; Huang, L. Amphipathic Polyethyleneglycols Effectively Prolong the Circulation Time of Liposomes. *FEBS Lett.* **1990**, *268*, 235–237.
30. Mishra, S.; Webster, P.; Davis, M. E. PEGylation Significantly Affects Cellular Uptake and Intracellular Trafficking of Non-viral Gene Delivery Particles. *Eur. J. Cell Biol.* **2004**, *83*, 97–111.